Desalination and Water Treatment 326 (2026) 101781

Contents lists available at ScienceDirect

Desalination and Water Treatment

journal homepage: www.sciencedirect.com/journal/desalination-and-water-treatment/

Optimization of operating and preparation parameters of TiO_2-$BiFeO_3$ nanoparticle-integrated PES membranes for dye removal

Hussain Ali Ibrahim [a], Khalid T. Rashid [a], Mohammed Ahmed Shehab [b], Mohammed A. Salih [c], Mohammad A. Taher [c], Haidar Hasan Mohammed [c], Mohammed Nabeel [d], Mahmood Alhafadhi [e,*], Adnan A. Abdul Razak [f]

[a] Membrane Technology Research Unit, College of Chemical Engineering, University of Technology, Al Sinaa Street 52, Baghdad 10066, Iraq
[b] Gas Processes and Petrochemicals Engineering Department, Basrah University for Oil and Gas, Basrah 61004, Iraq
[c] Department of Chemical Engineering and Petroleum Refining, Basrah University for Oil and Gas, Basrah 61004, Iraq
[d] Center of Industrial Applications and Materials Technology, Scientific Research Commission, Baghdad, Iraq
[e] Department of Mechanical and Energetic, University of Dunaújváros, Dunaújváros, Hungary
[f] Department of Oil and Gas Refining Engineering, Collage of Engineering, Al-Turath University, Baghdad, Iraq

HIGHLIGHTS

- TiO_2-$BiFeO_3$ NPs and PES MMMs are used in a novel way to simulate greasy wastewater and remove CR dye.
- To improve the method's efficacy on a wide scale, RSM and ANOVA were used.
- MMMs based on PES/TiO_2-$BiFeO_3$ demonstrated optimum efficiency with 44 kg/m^2 h flux and 99.88% CR dye rejection.

ARTICLE INFO

Keywords:
PES/TiO_2-$BiFeO_3$ membrane
Response surface methodology (RSM)
CR dye rejection
Analysis of variance (ANOVA)
Optimization

ABSTRACT

This work explores the optimization of poly (ether sulfone) (PES) mixed matrix membranes including titanium dioxide/bismuth ferrite (TiO_2–$BiFeO_3$) nanoparticles for improved dye-contaminated wastewater treatment. The manufacturing and operational factors that affect membrane compatibility, nanoparticle dispersion, and overall performance were emphasized. Within a central composite design framework, response surface methodology (RSM) in conjunction with analysis of variance (ANOVA) was used to methodically assess the effects of important variables, such as operating pressure (100–300 kPa), Congo Red (CR) dye concentration (0.1–0.3 g/L), and nanoparticle loading (0–0.1 wt%). Strong prediction ability was shown by the constructed model, which also found ideal conditions at 132 kPa operating pressure and 0.06 wt percent nanoparticle loading. In these circumstances, the membrane obtained a 99.88% CR dye rejection and a permeate flux of 44 $kg \cdot m^{-2} \cdot h^{-1}$. These results demonstrate the considerable potential of PES/TiO_2–$BiFeO_3$ mixed matrix membranes for advanced dye wastewater treatment applications by confirming their markedly improved permeability and separation efficiency.

1. Introduction

Wastewater containing dyes represents a serious environmental problem, especially because perceptions differ regarding the waste produced by industries such as textile processing, food manufacturing, paper and printing. Industrial processes discharge waste containing dyes, which, if untreated, may result in a variety of negative impacts on water usage and aquatic life [1]. High concentrations of dyes in water not only make it unsuitable for agricultural and household use, but they also interfere with light penetration, hindering the growth of aquatic plants that rely on light for food. The impact on plants also affects other organisms. They are also toxic substances that negatively affect the lives of fish. This pollution reaches humans through drinking contaminated

* Corresponding author.
E-mail addresses: che.23.17@grad.uotechnology.edu.iq (H.A. Ibrahim), Khalid.t.rashid@uotechnology.edu.iq (K.T. Rashid), mohammed.ahmed@buog.edu.iq (M.A. Shehab), mohammed.salih@buog.edu.iq (M.A. Salih), moh.may@buog.edu.iq (M.A. Taher), haidar.alawaad@buog.edu.iq (H.H. Mohammed), mohamedxl2006@gmail.com (M. Nabeel), Alhafadhi@uniduna.hu (M. Alhafadhi), adnansss2002@yahoo.com (A.A. Abdul Razak).

https://doi.org/10.1016/j.dwt.2026.101781
Received 16 March 2026; Received in revised form 17 April 2026; Accepted 27 April 2026
Available online 1 May 2026
1944-3986/

Nomenclature

Symbol / Abbreviation	
PES	Polyethersulfone—
TiO_2	Titanium dioxide—
$BiFeO_3$	Bismuth ferrite nanoparticles—
J	Permeate fluxkg·m^{-2}·h^{-1}
R	Dye rejection%
P	Operating pressurekPa
C_o	Initial dye concentrationmg·L^{-1}
C_p	Permeate dye concentrationmg·L^{-1}
t	Filtration timemin
A	Effective membrane aream^2
V	Volume of permeateL
ΔP	Transmembrane pressurekPa
wt%	Weight percentage of additives%
MMMs	Mixed Matrix Membranes—

water, bathing, consuming agricultural crops irrigated with contaminated water, or eating fish that live in polluted water bodies. Through these methods, the pollution reaches humans and can cause serious diseases that may lead to death. Textiles are notorious for the consumption of water which consumes a lot more water than any other industry [2].

This produced wastewater is characterized by high levels of pollution that require it to be properly treated before it is discharged. Dye wastewater emerges as a special concern because of the physio-chemical inability to break these products down. They have complex synthetic structures that allow them to resist light exposure, water, and different chemicals, which makes it hard to decompose them in nature. There are several categories of dyes namely, acidic, basic, disperse, azo, diazo, and metal complex all of which have their own base of difficulties in decolorization and breaking. These dyes may cause a lot of damage to the environment without proper treatment [3,4].

A major effort has been saved in innovative methods to remove dyes using membrane separation methods, biological therapies, photocatalysis, and adsorption and oxidation processes [5]. Traditional separation methods, including electrochemical, ozonation and hydrogen peroxide/UV methods, have however been found to be insufficient due to the complex aromatic nature; they are very impervious to deterioration. The dye compounds are especially resistant to the light conditions, oxidizing forces. Consequently, pressure-driven separation membrane processes have been gaining interest. They allow the possibility of reusing water and recovering valuable waste materials. Recent advancements in cost-effectiveness and technology have further solidified in the conception that membrane systems are indeed an option in the intensive treatment of industrial wastewater [6,7].

Membrane processes have become common in textile wastewater treatment because they have advantages over traditional processes [5]. However, any membrane processes must face a situation of reduced permeability flow due to the accumulation of contaminants on the surface of the membrane. Concentration polarization is the term for this phenomenon, which makes membrane fouling worse. To solve this problem, several solutions have been put forward, such as physical cleaning techniques and membrane surface alteration, operational process optimization, application of anti-fouling agents, hybrid membrane treatment, pre-treatment of raw water, enhanced cleaning methods, and dynamic membranes. These methods aim to alter the membranes' performance by improving their surface characteristics [8–10].

Nanomaterial-based surface modification has garnered significant interest due to its effectiveness in improving membrane performance and introducing hydrophilic properties. [11,12]. Nanomaterials like graphene oxide, zinc oxide, copper, silver, titanium dioxide, and carbon nanotubes, have been proven to overcome the limitations of traditional membrane processes [13]. It has been demonstrated that the use of nanofillers in polymeric membranes has increased the hydrophilicity, dye rejection, fouling resistance and thermal as well as mechanical stability [14,15].

It is interesting that adding several nanomaterials to a membrane structure has resulted in more improvement in membrane efficiency. It has been proven that these nano-additives not only modify the membrane's features but also possess new functions such as the photodegradation of pollutants accumulated on the membrane's surface. This keeps the membrane clean, allowing it to be used multiple times and extending its operational lifespan [16,17]. Zhang et al. also added TiO_2-Fe_2O_3 to a carbon membrane (CMs), improving its properties [18]. Li et al. also used a TiO_2/ZnO nanocomposite as an additive to a Polytetrafluoroethylene (PVDF) membrane [19]. Rathna et al. added TiO_2-WO_3 to the Polyaniline (PANi) membrane matrix [20]. All these composite additives significantly enhanced the membranes' properties rejection properties and improved pure water permeability. In addition, these membranes possess another advantage: photocatalytic properties that can clean the membrane surface of accumulated contaminants. This prolongs the membrane's operational life and reduces costly cleaning operations that can damage the membrane. Although the development of nanocomposite membrane fabrication is advanced, balancing the operation variables is pivotal to an efficient application of the membrane fabrication. The best operation conditions will reduce membrane fouling and improve effectively, the membrane properties and life span. Given the numerous parameters and interactions that affect the efficiency of the membrane, the design of experiment (DOE) technique has the capacity to largely address the solution so that the desired outcomes can be attained. Response surface methodology (RSM) is such a potent example that is used towards maximum optimization of process parameters [21,22]. RSM is a very good tool in the reduction of the number of process variables and tests optimization to incur the least amount of time and material cost. It yields outcomes which are especially probable and powerful and are statistically predicted [23,24]. RSM as a mathematical-statistical tool can consider the interactions of several factors and provide the process of membrane application with significant enhancement in case it is compared to the method of one-factor at a time. Consequently, RSM establishes correlation between variables and their effects on any one or more measured responses in addition to providing the most appropriate level of a given variable [25,26]. For instance, Karunakaran et al. employed response surface methodology (RSM) combined with central composite design (CCD) to evaluate the influence of key operating parameters, Cr concentration (0.1–0.9 ppm), pH (2–6), and pressure (approximately 1–5 kg cm^{-2}) on membrane performance. The optimum conditions were determined to be 400 kPa, pH 3, and a Cr concentration of 0.431 ppm [27]. In another study, Srivastava et al. applied response surface methodology (RSM) to optimize key operating factors influencing salt rejection, water flux, and permeate recovery in a nanofiltration (NF) system. The model was validated using analysis of variance (ANOVA). Feed concentration (3500–6500 mg L^{-1}), pressure (5–9 kg cm^{-2}), and pH (5.5–8.5) were considered as independent variables. The optimal conditions were determined to be 6500 mg L^{-1}, 9.4 kg cm^{-2}, and pH 6.8 [28].

By adopting a methodical and quantitative optimization methodology, the current study expands on our earlier work [29], which mainly showed the manufacture, characterisation, and initial viability of the proposed membrane for Congo Red (CR) dye removal. In particular, this work uses statistical modeling and controlled experimental design to clarify the combined impact of important operational and fabrication parameters, specifically feed concentration, transmembrane pressure, and additive loading. This study is unusual because it uses an integrated strategy to simultaneously optimize several interacting variables, which allows for the identification of ideal operating conditions and the discovery of the underlying mechanisms controlling fouling behavior, rejection efficiency, and permeation. This work offers quantitative insight into parameter interactions and their synergistic effects, providing a more realistic portrayal of membrane performance under practical conditions, in contrast to previous research that concentrate on single-factor analysis or preliminary performance evaluation. By providing practical design and operational instructions, this study ultimately closes the gap between material development and process implementation, improving process stability, scalability, and efficiency for the treatment of dye-contaminated wastewater.

2. Experimental work

2.1. Materials

Solvay Advanced Polymers in Belgium is the source of Polyethersulfone (PES). Sigma-Aldrich company (Germany) was the one that supplied the N, N-Dimethylacetamide (DMAc), Ethylene glycol (EG) and Titanium dioxide (TiO_2) NPs. DMAc was used as a solvent for polyethersulfone (PES), CR dye, which used as a wastewater contaminate were obtained from Shandong Jiurunfa Chemical Technology Co., Ltd. Ethanol (EtOH) was obtained from VWR International Ltd., Hungary. From C.E.R., France, Iron nitrate nonahydrate [Fe $(NO_3)_3 \cdot 9H_2O$] and bismuth nitrate pentahydrate [Bi $(NO_3)_3.5H_2O$] were obtained.

2.2. Preparation of TiO_2-$BiFeO_3$ (TBF) nano-additive

TiO_2–$BiFeO_3$ nanoparticles were prepared as shown in Fig. 1. The initial solution was created by dissolving a fixed quantity of bismuth nitrate [$Bi(NO_3)_3 \cdot 5H_2O$] in ethanol (EtOH). The second solution was obtained by dissolving iron nitrate [$Fe(NO_3)_3 \cdot 9H_2O$] in ethylene glycol (EG). To guarantee uniform dispersion, a predetermined quantity of TiO_2 nanowires (TiO_2 NWs) was next added to the initial solution while being continuously stirred magnetically. Then, while continuously stirring, the second solution was progressively added to the first until a homogenous mixture was obtained. The resultant mixture was put into a stainless-steel autoclave lined with Teflon. Utilizing a Teflon liner ensures product purity by minimizing contamination, preventing chemical interaction with the reaction medium, and withstanding high temperatures and pressures. After being sealed and heated to 180 °C for 24 h, the autoclave naturally cooled to ambient temperature (20 ± 2 °C). To get rid of any remaining ions and contaminants, the reaction's product was carefully cleaned using ethanol and deionized water. Filtration or centrifugation were used to separate the material after it had been repeatedly dispersed in the solvent during the washing procedure. Until a neutral pH (~7) was reached, this process was repeated at least three times, showing that the contaminants had been successfully removed. After drying, the refined product was calcined for two hours at 500 °C to improve crystallinity and remove any last traces of organic matter. The final TiO_2–$BiFeO_3$ nanocomposite was obtained by drying the powder in an oven for 12 h to eliminate any remaining moisture and stop nanoparticle aggregation.

2.3. Membrane preparation

Through our previous research, the method for preparing the membranes was explained [27]. In summary, the membrane solution was prepared, which consists of a solvent (DMAc), then we add the polymer (PES), and finally the nanomaterial (TiO_2-$BiFeO_3$). We mix the mixture well, then pour it onto a casting knife and cast the membrane solution onto a glass plate. After that, we immerse the glass plate in water until the sheets separate. Then we store the membrane in containers containing distilled water. This process is called phase inversion, where the membrane transitions from a liquid state to a solid state because water expels the solvent or an exchange occurs between water and the solvent. This exchange process forms the pores and causes the membrane to

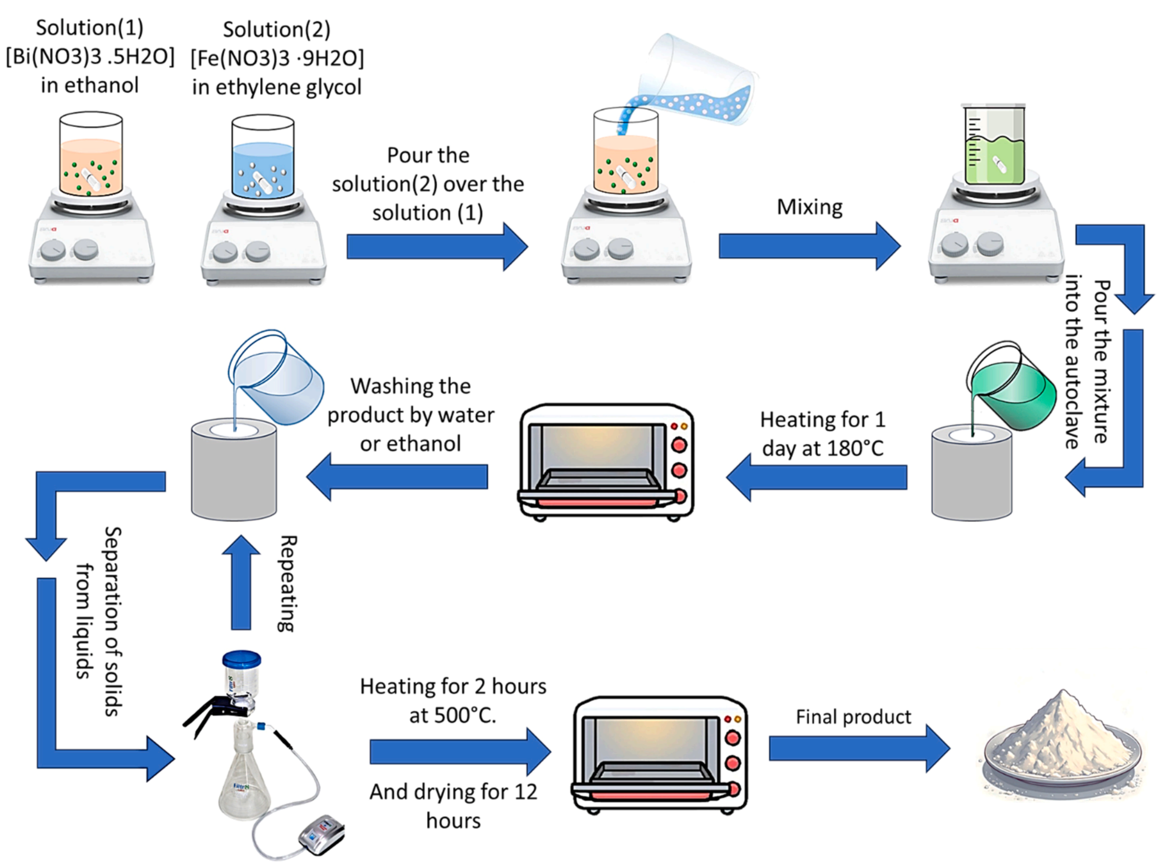

Fig. 1. Preparation of TiO_2-$BiFeO_3$ nano additive.

transition to a solid state. Before adding the substance, we must grind it to a nanoscale size so that we can add it to the membrane solution. Because particles with large sizes have a weak bond with the membrane, they are removed by water during immersion in the water basin. This can lead to holes or voids in the membrane, resulting in inaccurate performance results because water will pass through these voids instead of the pores, and also a decrease in the separation efficiency of pollutants. Table 1 shows the proportions of the materials used in the preparation process. Fig. 2 shows the preparation method.

2.4. Membrane performance

The pure water flux (PWF) for PES /TiO_2-$BiFeO_3$ membranes and pure membrane were measured by filtration system Scheme 1. [27]. The area of effective membrane filtration was 0.002304 m^2. All the membranes were operated (Scheme 1) with pure water at least 10 min under 250 kPa till a steady flux was reached before proceeding to run filtration experiments. The water permeability measurements were repeated thrice to give accurate results, and the mean values were recorded. Given that the flux is in Kg/m^2 h, the equation below was used to compute the flux.

$$\text{PWF} = \frac{\boldsymbol{Q} * \quad \boldsymbol{\rho}}{\boldsymbol{A}} \tag{1}$$

Where Q is volumetric flowrate (m^3/ hr.), ρ is density of water (kg/m^3) and A is the area of effective membrane filtration (m^2)

Congo red (CR) dye was chosen in the present research as a model contaminant to be used in determining the performance of the membrane. This filtration was done under a constant PH of 7 and a temperature of 30 C, and the dye solutions were used at concentrations of 100, 200 and 300 mg/L and operating pressure (100,200,300) kPa. Similarly, the action of the nano additive amount that was used in the prepared membranes was tested. Using UV-Vis. spectrophotometry, dye content of the permeate and feed stream was determined at a wavelength of 498 nm. Dye rejection efficiency of membranes was estimated using the formula that follows:

$$\text{R}(\%) = \frac{\boldsymbol{C_T} - \boldsymbol{C_B}}{\boldsymbol{C_T}} \times 100\% \tag{2}$$

Where R is the dye rejection %, C_B and C_T are the dye feed and permeate concentration streams, respectively

3. Simulations

Design-Expert software was exploited in the study to design and analyze the experiment. The principle used was to utilize data response surface methodology (RSM) design to associate and design three main operation variables that influenced the membrane flux and retention. A historical data RSM design was implemented to connect and optimize three key operation parameters influencing the flux and rejection efficiency of the control and modified membranes. The historical data design approach permits flexible selection of experimental data points, making it particularly advantageous when working with pre-existing data [30–32]. The design of data does not have any limitation to the number of factors that may be used in its design unlike any other kind of RSM design, and it has eased the process of conducting unlimited analysis and auditing of the membrane achievement. In this work, three critical operational parameters affecting the flow and rejection efficiency of the neat and modified membranes were connected and optimized using a historical data RSM design. The historical data design technique is especially useful when dealing with pre-existing data since it allows for variable selection of experimental data points. In this case, the three independent variables were investigated as (A) Congo red (CR) concentration (100, 200 and 300 mg/L), (B) TiO_2-$BiFeO_3$ (0–0.1%. wt.) and (C) pressure level (100, 200 and 300 kPa) (Table 2). The effect of these parameters on dye rejection efficiency and membrane flux was systematically studied with the help of RSM. The ideal conditions were set depending on the data obtained.

Researchers often utilize the analysis of variance (ANOVA) to establish how independent factors affect dependent parameters in regression research, a series of statistical terms of analyzing the variations among multiple parameters. An experimental study was done in a sequence of tests using the UF membrane system where each test varied one variable and kept the other variables constant to establish the operating conditions that would be required. Table 1. summary of operating parameters and experimental conditions for membrane performance evaluation. RSM was deployed as the method of optimization to examine the influence of different variables on the process of a membrane performance Table 2**.** presents the key independent and dependent variables considered in the membrane filtration experiments. The operating parameters include transmembrane pressure, additive loading, and initial dye concentration, which were systematically varied within the specified ranges to evaluate their influence on membrane performance. Table 3. summarizes the independent process variables used in the Response Surface Methodology (RSM) experimental design, along with their coded representations and corresponding actual levels. The studied factors include initial dye concentration (A), additive loading (B), and operating pressure (C), each varied within defined low and high levels to evaluate their individual and interactive effects on membrane performance. These coded variables were used to develop and analyze the statistical model for process optimization. Table 4 illustrates the historical data on the 18 tests that were carried out. The data gave the essential design parameters of the modeling and optimization of the permeate flux and dye retention.

PBIAS (Percent Bias) is calculated using the following formula:

$$PBIAS = 100 \quad x\ \frac{\sum(O_i - S_i)}{\sum Q_i} \tag{3}$$

Where Q_i = actual values

S_i = Predicted values from the model

If PBIAS = 0 → the model is perfectly accurate

If it is positive → the model underestimates the actual values

If it is negative → the model overestimates the values

The PBIAS values for rejection and flux close to zero indicate high models accuracy.

4. Results and discussion

4.1. Membranes' performance

In terms of dye rejection and pure water flux (PWF), each PES/TBF membrane fared better than the basic membrane. The flow parameters were significantly affected by the addition of the TBF NP additives. The findings showed that when 0.025 wt% of TBF NPs was added, the water flow increased from 8.246 (Kg/m^2 h) for the original membrane to 25.6 (Kg/m^2 h). The PWF for Ĥ2 rose dramatically with the addition of TBF NPs; the maximum value was 46.44 (Kg/m^2 h). As seen earlier, the increase in PWF matched measures of the produced membrane's hydrophilicity, porosity, and pore size. Notably, the pure water flow decreased to 34.739 (Kg/m^2 h) when 0.075 wt% of TBF NPs was added, and

Table 1
Proportions of materials used in the membrane preparation process.

Membrane Code	PES (wt%)	TiO_2–$BiFeO_3$ (TBF) (wt%) *10^2	DMAC (wt%)
Ĥ0	18	0	82
Ĥ1	18	2.5	81.975
Ĥ2	18	5	81.95
Ĥ3	18	7.5	81.925
Ĥ4	18	1	81.9

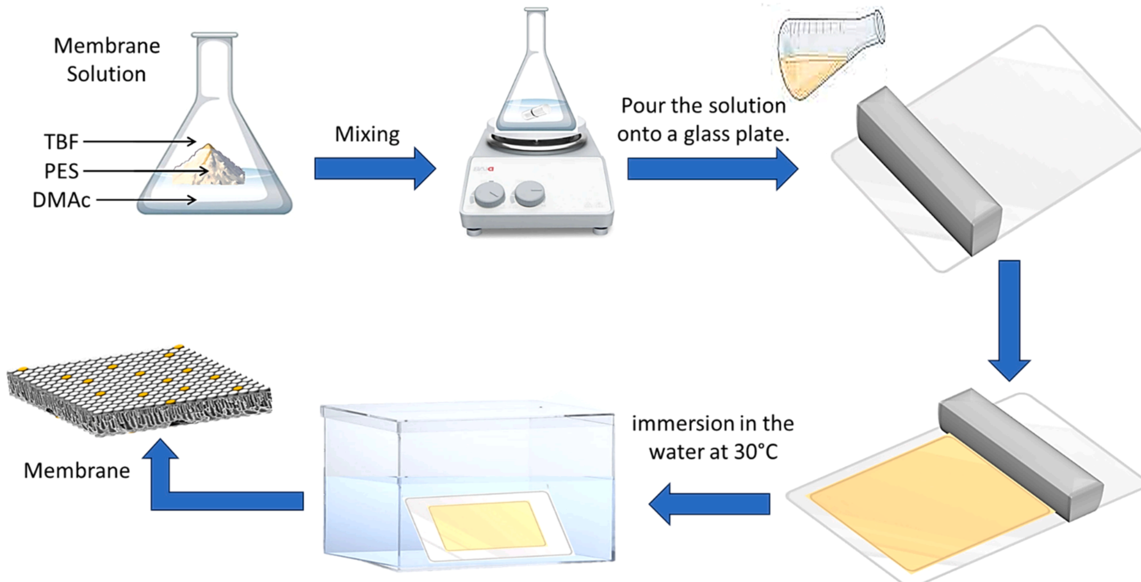

Fig. 2. Method of preparing membranes.

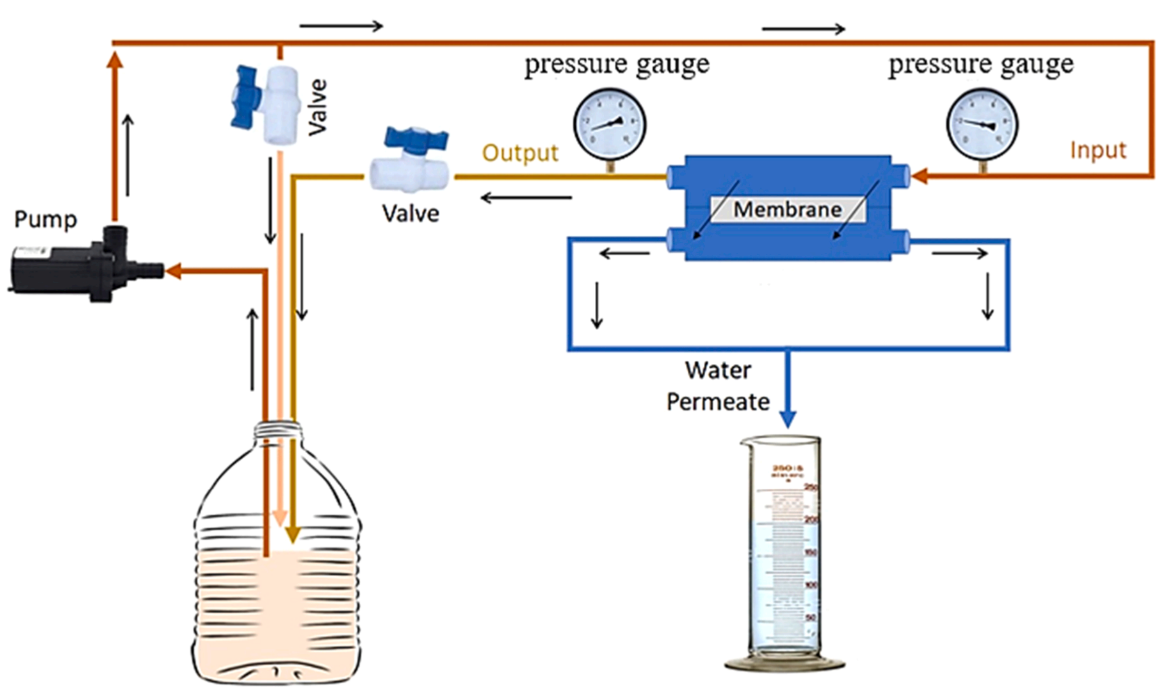

Scheme 1. Diagrammatic representation of the UF cross-flow system.

subsequently to 26.38 (Kg/m^2 h) when the TBF load percentage rose to 0.1% wt%. Due to pore constriction caused by the elevated PRS NP concentration, the PWF dropped. The aggregation events caused by the elevated TBF content in the casting fluid reduced the membranes' performance.

4.2. Analysis using ANOVA

ANOVA analysis was carried out using Design-Expert®. Table 5 and Table 6, which present the measurements of transmembrane pressure and dye concentration illustrate the outcomes of the (ANOVA) analysis of the PWF and the percentage dye retention taking into consideration the TBF NP content. Every predictor variable is linked to a certain p-value in the outcomes table of ANOVA in the design layout. The results were checked to come up with a mathematical term. Regression model equations in terms of the permeate flux and the percentage rejection are given as below in the form of Eqs. (4) and (5) in terms of the real parameters with respect to the membranes.

$$\text{Flux (kg/m}^2\text{. h)} = +48.84 - 1.64\,A + 6.19\,B + 11.40\,C - 0.92\,AB + 3.35\,BC + 0.11\,A^2 - 32.43\,B2 + 3.72\,C^2 \quad (4)$$

$$\text{Rejection (\%)} = +93.92 - 2.91\,A + 8.47\,B - 6.19\,C + 1.25\,AB + 2.35\,BC - 0.23A^2 - 8.82\,B^2 - 2.51\,C^2 \quad (5)$$

Terms with positive factors in Eq. (3) represent a positive influence on the flux and negative part represent a negative impact. The factor term in Eq. (4) has a positive value, means that it has a positive influence on the rejection whereas a negative value means that it has a negative

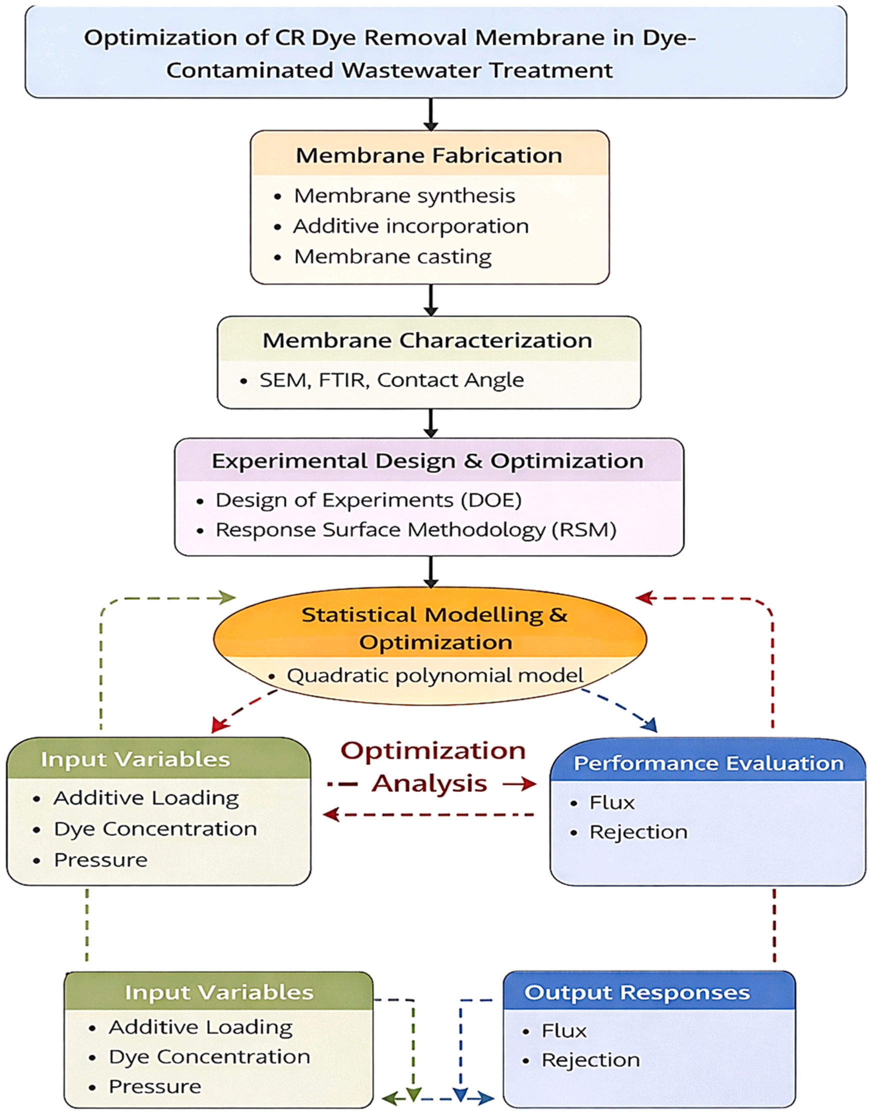

Scheme 2. Study flow chart (Schematic diagram).

Table 2
Summary of operating parameters, membrane characteristics, and performance responses used in the experimental study.

Parameter	Symbol	Range / Value	Unit
Operating pressure	P	100 – 300	kPa
Additive loading	wt%	0 – 0.10	wt%
Initial dye concentration	C_0	100–300	mg·L^{-1}
Permeate flux	J	Measured	kg·m^{-2}·h^{-1}
Dye rejection	R	Measured	%
Membrane type	—	PES-based MMM	—

Table 3
Factor levels and parameter codes.

Parameters	Coded	Unite	Low level	High level
Dye concentration	A	mg/L	100	300
TBF	B	% wt%	0	0.1
Pressure	C	kPa	100	300

influence.

According to the adjusted R-squared values, the permeate flow and rejection percentage models' R-squared correlation coefficients were 99.73% and 99.16%, respectively, and 99.49% and 98.41%. Computed values of the R squared were satisfactory to show similarity of the results tested with the values of optimization. According to the data, PWF model and dye rejection % model was statistically acceptable and could be used to predict the behavior of UF system.

Regression analysis of the PWF and % rejection models revealed that the model was very accurate and was well represented in the given data [33]. The expected values of R-squared correlation coefficient (predicted) were nearly equal to the values of R-squared adjustment correlation coefficient as indicated in Table 5 and Table 6. Therefore, in both models, important terms were involved. Design Expert(r) software was used to estimate the flux and percentage of rejection by a linear regression algorithm. Actual and expected results of the permeate flux and the rejection percentage are depicted in Fig. 3. Both the results of the real and forecasted values of PWF and the % rejection showed a significant mathematical agreement, as demonstrated in Fig. 3 A and B. Above outcome and the high values of the R-squared (99.78% and 9.36% of the PWF and rejection percentage, respectively) of the (PES/TBF) membrane revealed that the model has a strong predictive and optimization capacity of the permeate flux and the percentage rejection of the permeate [34].

Table 4
Experimental and response data points.

Runs	A: Initial dye con. (ppm)	B: Additions loading (wt%)	C: Pressure (kPa)	Rejection %	Predicated	$(O_i - S_i)$	Flux (kg/m^2. h)	Predicated	$(O_i - S_i)$
1	100	0	200	82.1	80.56	1.54	12.78	11.069	1.711
2	200	0	200	76.28	76.63	-0.35	11.09	10.230	0.86
3	300	0	200	71.61	72.23	-0.62	8.77	9.617	-0.847
4	100	0.05	200	96.11	96.596	-0.486	49.86	50.599	-0.739
5	200	0.05	200	94.07	93.921	0.149	49.36	48.844	0.516
6	300	0.05	200	92.3	90.778	1.522	47.89	47.314	0.576
7	100	0.1	200	95.87	94.989	0.881	24.52	25.276	-0.756
8	200	0.1	200	93.77	93.568	0.202	21.23	22.605	-1.375
9	300	0.1	200	90.78	91.679	-0.899	20.43	20.159	0.271
10	100	0	100	86.6	86.595	0.005	7.012	6.745	0.267
11	100	0	200	80.7	80.56	0.14	9.812	11.069	-1.257
12	100	0	300	68.8	69.51	-0.71	22.1	22.835	-0.735
13	100	0.05	100	99.4	100	-0.6	42	42.921	-0.921
14	100	0.05	200	95.74	96.596	-0.856	50.085	50.599	-0.514
15	100	0.05	300	88.45	87.898	0.552	66.8	65.718	1.082
16	100	0.1	100	97.2	96.423	0.777	14.9	14.246	0.654
17	100	0.1	200	93.77	94.989	-1.219	26.83	25.276	1.554
18	100	0.1	300	88.8	88.641	0.159	43.402	43.749	-0.347
$\sum$				1592.35		0.187	528.871		-7.1E-15

Table 5
Membranes flux by ANOVA.

Source	Sum of Squares	df	Mean Square	F Value	p-value Prob > F	
Model	5687.9900	8	711.0000	412.8000	< 0.0001	significant
A-Initial dye con.	21.5800	1	21.5800	12.5300	0.0063	
B-Additions loading	321.6000	1	321.6000	186.7200	< 0.0001	
C-Pressure	779.5300	1	779.5300	452.5900	< 0.0001	
AB	5.8800	1	5.8800	3.4100	0.0978	
BC	44.9800	1	44.9800	26.1200	0.0006	
A^2	0.02700	1	0.02700	0.01600	0.9022	
B^2	205.8300	1	4205.8300	2441.8600	< 0.0001	
C^2	41.5400	1	41.5400	24.1200	0.0008	
Residual	15.5000	9	1.7200			
Lack of Fit	8.4000	6	1.4000	0.59	0.7325	not significant
Pure Error	7.1000	3	2.3700			
Cor Total	5703.4900	17				
Std. Dev.	1.3100		R-Squared		0.9973	
Mean	29.3800		Adj R-Squared		0.9949	
C.V.%	4.4700		Pred R-Squared		0.9884	
PRESS	66.0100		Adeq Precision		63.548	

Table 6
Rejection% of membranes by ANOVA.

Source	Sum of Squares	df	Mean Square	F Value	p-value Prob > F	
Model	1381.8200	8	172.7300	132.8300	< 0.0001	significant
A-Initial dye con.	67.7100	1	67.7100	52.0700	< 0.0001	
B-Additions loading	602.4500	1	602.4500	463.3100	< 0.0001	
C-Pressure	230.0200	1	230.0200	176.8900	< 0.0001	
AB	11.0100	1	11.0100	8.4700	0.0173	
BC	22.0900	1	22.0900	16.9900	0.0026	
A^2	0.1200	1	0.1200	0.09200	0.7685	
B^2	311.2900	1	311.2900	239.3900	< 0.0001	
C^2	18.8500	1	18.8500	14.5000	0.0042	
Residual	11.7000	9	1.3000			
Lack of Fit	8.4500	6	1.4100	1.3000	0.4486	not significant
Pure Error	3.2500	3	1.0800			
Cor Total	1393.5300	17				
Std. Dev.	1.1400		R-Squared		0.9916	
Mean	88.4600		Adj R-Squared		0.9841	
C.V.%	1.2900		Pred R-Squared		0.9547	
PRESS	63.1000		Adeq Precision		38.1600	

4.3. Independent factors' effects on permeate flux and rejection

Fig. 4 shows how Design-Expert(r) software was used to analyses the impact of the experimental variables and their interactions. When the slope has a value, it indicates the strength of its effect, and the higher the slope's value, the greater its effect. In this experiment, one variable is

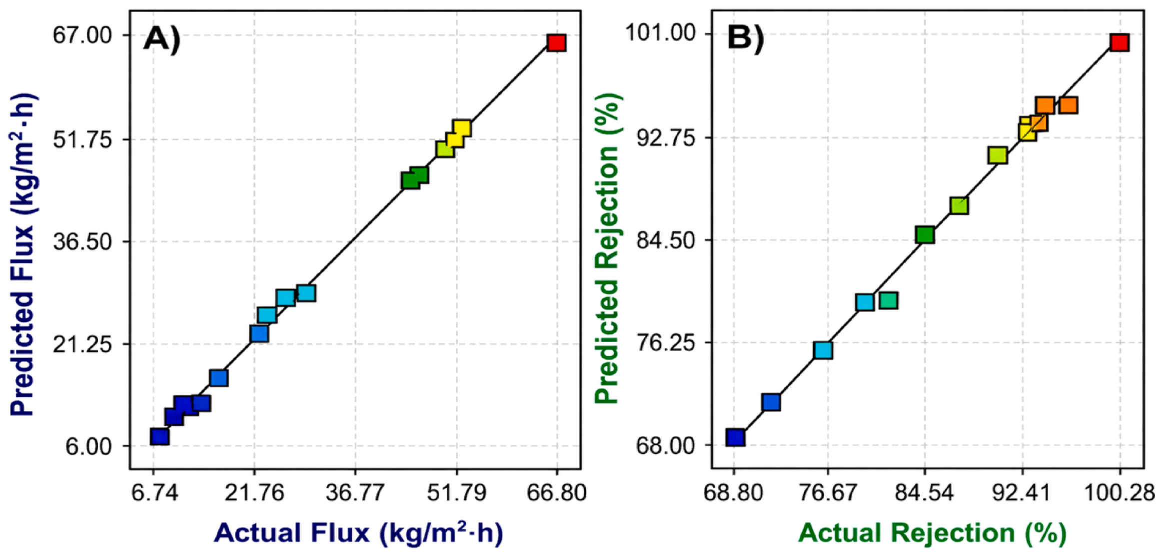

Fig. 3. Actual and predicted outcomes for the rejection percentage (B) and membrane flux (A).

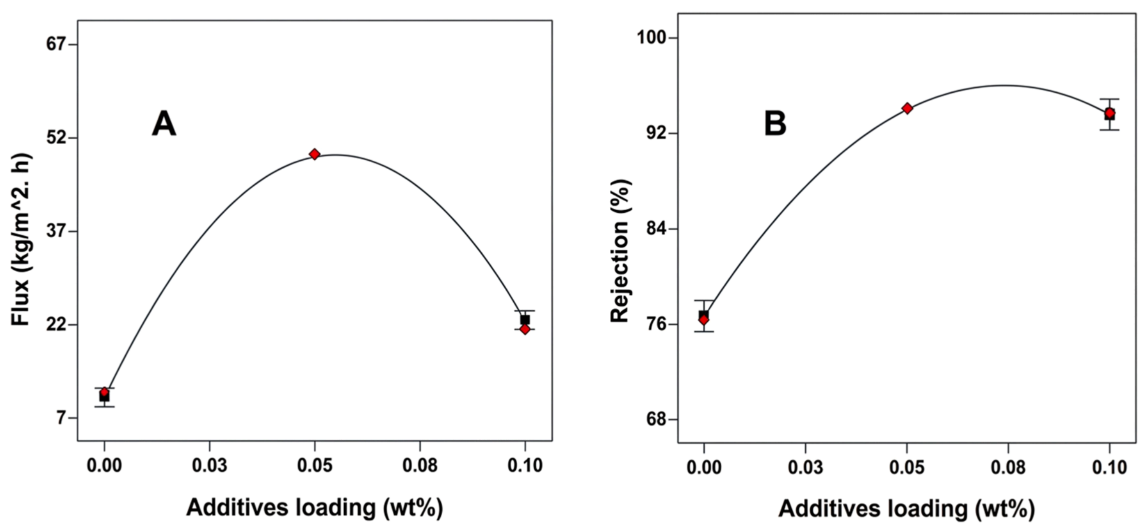

Fig. 4. Additives loading effect on A) flux and B) rejection (%) for membranes with steady CR dye conc. 0.2 g/L, and pressure 200 kPa.

changed while the other variables are kept constant [35,36]. Fig. 4 (A) and (B) show the effect of TiO_2-$BiFeO_3$ content on permeate flux and % rejection at a steady pressure of 200 kPa with dye feed concentration of 0.2 g/L. Rising the additive content from 0 to 0.1 wt% led to enhanced rejection and flux of membrane. This improvement is due to the increased porosity of the membrane, the average pore size and the hydrophilicity, which increase the water permeability and the successful rejection of dyes. These observations are in line with the earlier studies that showed that the use of nanomaterials in polymeric membranes increases their permeability and selectivity based on the modification of surfaces and structural rearrangements.

Fig. 5 represents the effect of dye concentration on permeate flux and % rejection of membranes with constant pressure 200 kPa and additive concentration of TBF is 0.05%. wt. The flux and rejection efficiency decreased with increase in dye concentration, from 100 to 300 mg/L. The explanation of this decrease in flux is due to the accumulation of dye molecules on the membrane's surface, creating a thin compact layer that prevents water permeability. And the decrease in concentration can also be caused by concentration polarization, as we explained previously in our previous work [27].

Fig. 6 demonstrates the impact of pressure on membrane flow and rejection where TBF concentration was fixed at 0.05%. wt. and the dye concentration at 200 mg/L. As the operating pressure is increased by 100 kPa to 300 kPa of filtration membranes the permeate flux increases because the stronger driving force acts to propel the water through the membrane pores as the higher pressure surpasses the hydraulic resistance to permit a larger volume of liquid to flow at a given time. This rise in flux usually, however, comes at the price of lowering rejection efficiency, as the increased pressure increases the polarization of concentration at the surface of the membrane, and increases the probability of smaller solutes or contaminants to be passed through the pores. It can also in certain instances result in minor expansion of the pores or the extra strain on the active layer, decreasing the accuracy of the membrane in separation. Therefore, the correlation between pressure, flux and separation represents a balance act between the hydraulic driving force and membrane selectivity.

4.4. Effect of pressure dye concentration, TiO_2-$BiFeO_3$ (TBF) additives on membrane flux and %rejection

It can be described the three-dimensional solids for the dye response flux and the dye rejection percentage. Fig. 7-S1 are a graphical

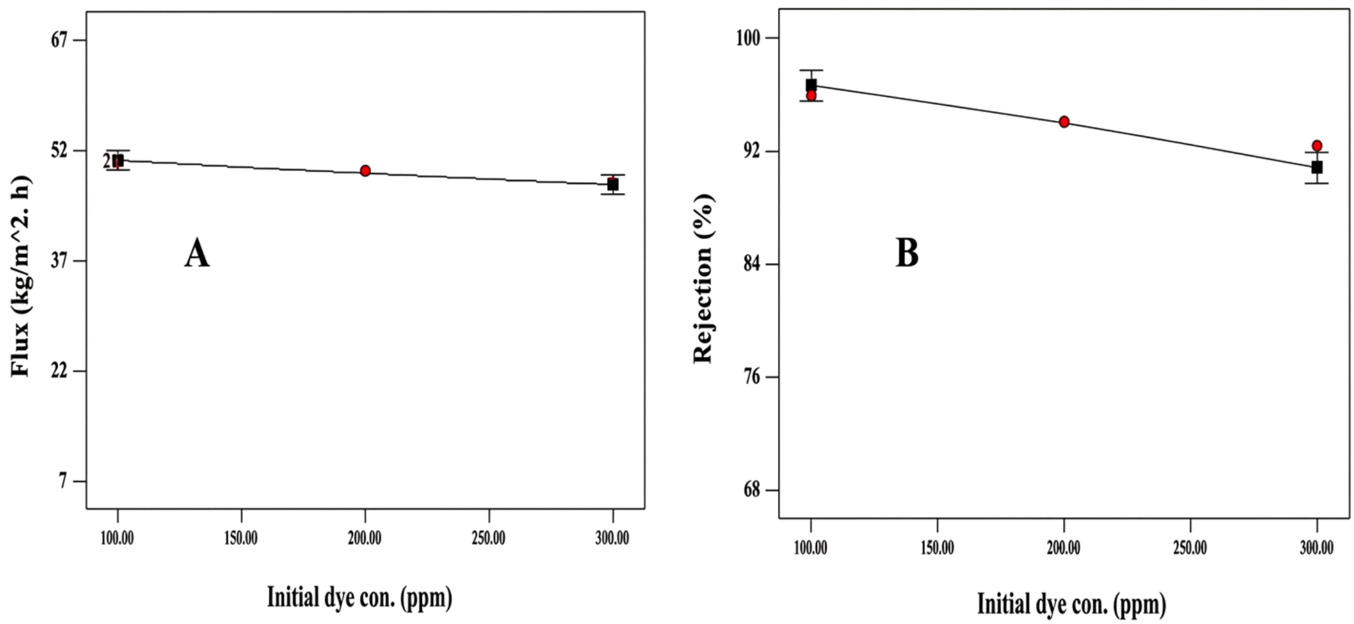

Fig. 5. The CR dye conc. influence on A) flux and B) rejection % for membranes at steady pressure 200 kPa, additives loading 0.05 wt%.

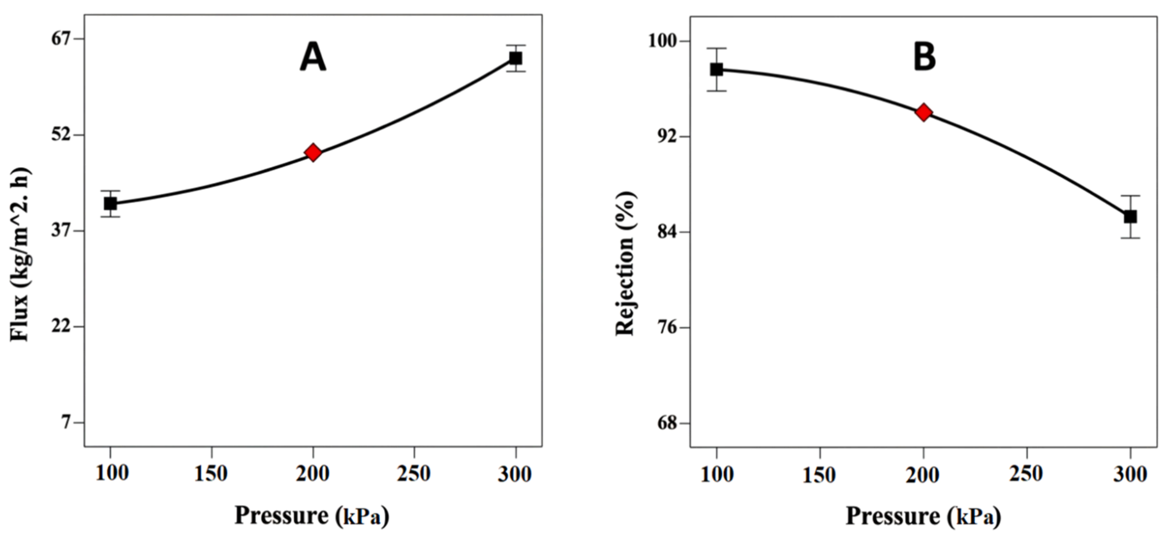

Fig. 6. Transmembrane pressure effect on A) flux and B) rejection (%) for membranes at steady CR dye conc. 200 mg/L, additive loading 0.05 wt%.

representation of the flux and the dye % rejection depending on the two parameters. The key goal of the plot of response surface was to determine the best conditions, particularly the dyes concentration, additives content and operation pressure that would result in the highest membrane performance.

The response surface analysis of dye rejection and permeate flux as a function of initial dye concentration and additive loading at a constant pressure of 200 kPa is shown in Fig. 7**.** The close distribution of experimental points around the expected response and the smooth curvature of the surfaces show that the derived quadratic model agrees well with the experimental data. The model's significance was validated by statistical analysis (ANOVA), which shows that membrane performance is significantly influenced by both primary components and their interaction terms [37]. Both answers have a strong nonlinear tendency, indicating the presence of optimal operating regions as opposed to straightforward linear relationships. Flux (Fig. 7A) increases initially with additive loading because of better pore shape and membrane hydrophilicity; however, flux decreases after an ideal loading because of increased transport resistance or pore blockage. Concentration polarization and the creation of fouling layers on the membrane surface can be linked to the simultaneous decrease in flow caused by an increase in dye concentration [38]. Rejection, on the other hand, shows an increasing trend with additive loading up to an optimal level (Fig. 7B), indicating greater electrostatic or size-exclusion effects and improved selectivity. However, rejection tends to somewhat diminish at greater dye concentrations, perhaps as a result of enhanced solute transport via the pores and membrane saturation. The interaction between the variables also shows that performance is constrained under highly concentrated feed conditions, whereas the influence of additive loading is more noticeable at lower dye concentrations. All things considered, the model accurately depicts the intricate relationship between fabrication and operating parameters, offering trustworthy forecasts within the examined range. However, it should be highlighted that the model is empirical and that its application is limited to the parameter domain under investigation; therefore, additional validation is required before extrapolating to industrial-scale settings.

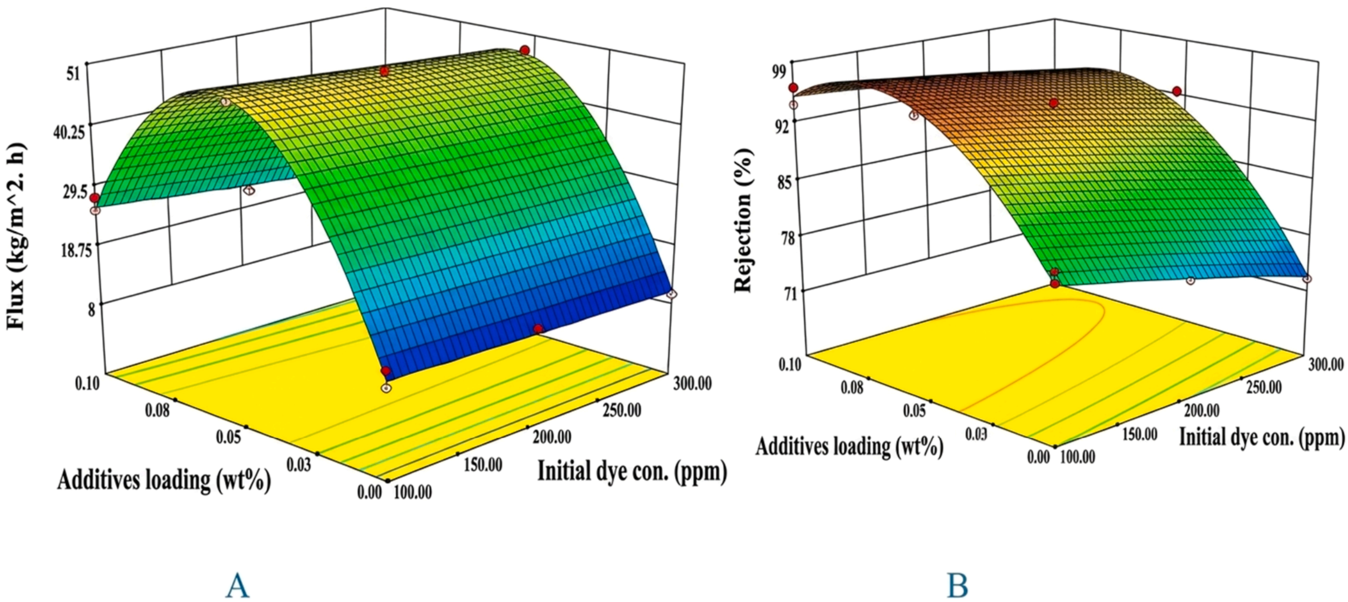

Fig. 7. A) flux and B) rejection (%) at pressure 200 kPa as a function of dye and additive concentrations.

Fig. 8 depicts the combined effects of operating pressure and initial dye concentration on (A) permeate flux and (B) dye rejection in the produced membranes. As illustrated in Fig. 8A, the permeate flux increases significantly with increasing pressure, rising from roughly 38–42 kg·m^{-2}·h^{-1} at 100 kPa to about 62–67 kg·m^{-2}·h^{-1} at 300 kPa, depending on the dye concentration. This tendency is due to the increased transmembrane driving force, which promotes water penetration. In contrast, increasing the initial dye concentration from 100 to 300 ppm results in a gradual decline in flux (approximately 10–15% reduction), which can be explained by increased solution viscosity and the development of concentration polarization and fouling layers that hinder mass transfer [39,40].

As shown in Fig. 8B, dye rejection improves with increasing initial dye concentration, rising from roughly 88–91% at 100 ppm to around 97–99% at 300 ppm. This boost is linked to higher solute-membrane contacts and the creation of a denser cake layer, which improves selectivity. Increasing pressure enhances rejection marginally, especially at lower concentrations. However, at higher pressures (about 300 kPa), rejection plateaus, indicating a limitation in separation efficiency. Overall, these findings show that, while increased pressure greatly increases flow, optimal dye rejection occurs at higher dye concentrations, emphasizing the importance of balancing operating conditions for maximum membrane performance [41,42].

The combined effects of operating pressure and nanoparticle additive loading on (A) permeate flux and (B) dye rejection of the modified polyethersulfone membranes are shown in Fig. 9. Because of the increased pushing force across the membrane, the permeate flux increases dramatically with increasing pressure, as seen in Fig. 9 a. Nevertheless, the flow shows a non-linear pattern at greater additive loadings, where an ideal concentration of nanoparticles enhances membrane porosity and hydrophilicity, making water transfer easier. Excessive nanoparticle incorporation after this point may result in pore blockage or increased structural resistance, which would cause flow to slightly decrease [43,44]. In contrast, Fig. 9 B shows that dye rejection improves with increasing additive loading, which can be attributed to increased surface functionality, smaller pore size, and better interaction

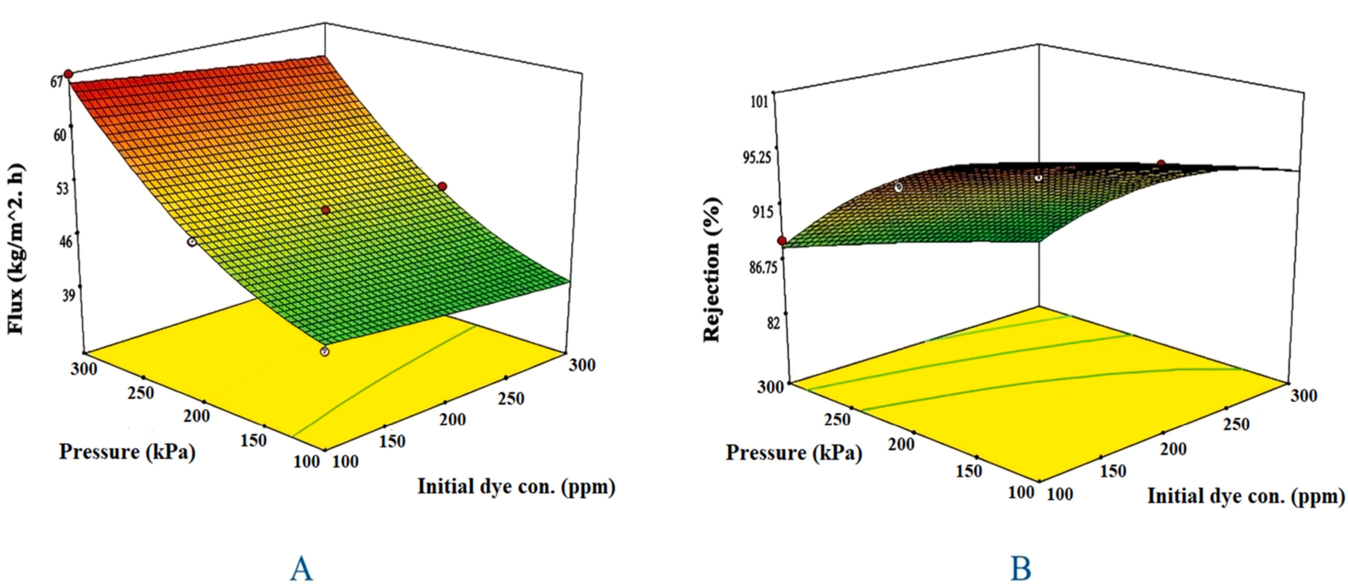

Fig. 8. Impact of starting dye pressure and concentration on A) flux and B) rejection (%) at 0.05 wt% percent additive loading.

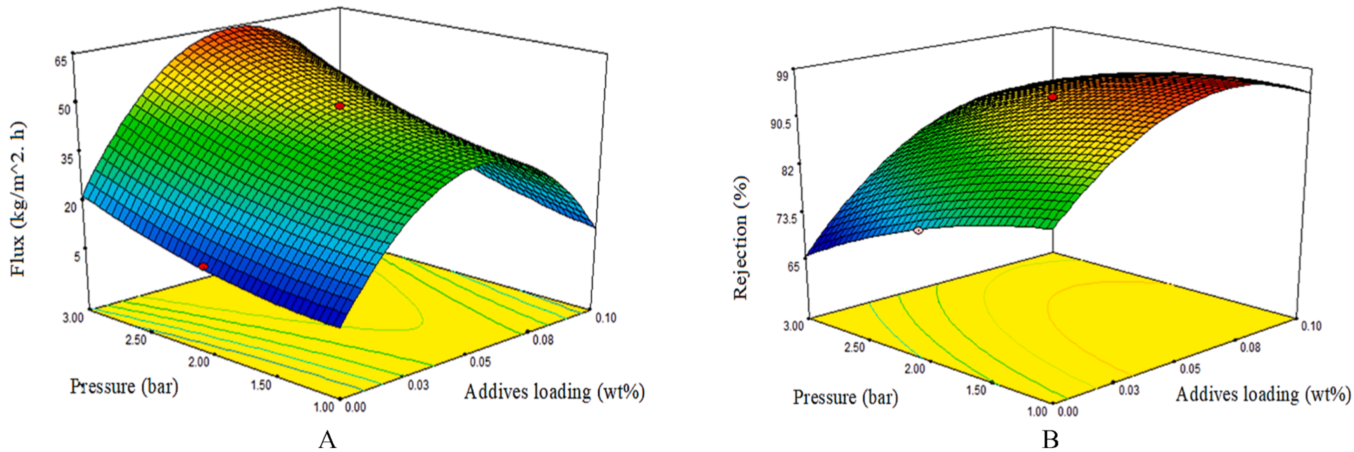

Fig. 9. A) flow and B) rejection (%) of prepared membrane at an initial dye concentration of 200 mg/L as a function of pressure and additive loading.

between the membrane surface and dye molecules. Furthermore, increasing pressure marginally improves rejection due to enhanced solute-membrane interactions; however, at very high pressures, the effect diminishes due to membrane pore deformation. Overall, the results show that both pressure and additive loading have a synergistic effect, and an optimal balance of both factors is required to achieve high flux and dye rejection performance. Increasing the additive loading improves the membrane properties and enhances its selectivity, raising the rejection from about 65% in the absence of additives to nearly 99% at higher loadings (0.08–0.10 wt%). This indicates that the best performance can be achieved at an appropriate additive loading combined with moderate operating pressures [45,46].

4.5. Optimization and model validation

The optimization performed indicated the most desirable working conditions to be achieved with a dye concentration of about 125 mg/L, an additive loading of 0.06 wt%, and an operating pressure of 132 kPa as in Fig. 10. The model in these circumstances gave a rejection of 99.82% and a flux of 43.83 kg/m^2 h. Experimental validation of these conditions yielded 98.2% rejection and 44 kg/m^2 h, demonstrating the model's accuracy (error $<$ 1.6%) (Table 7). The "accuracy" in this context corresponds to the model's predictive capability, which is reflected by the high desirability value (Desirability = 1.000), indicating an excellent agreement between predicted and experimental responses. The distribution and interaction of experimental points used to build the model control the change in accuracy with regard to the dataset. In particular:

- Because of the sufficient number of experimental runs and appropriate coverage of variable ranges, the model exhibits high accuracy within the analyzed design space.
- The region where the regression model attains maximum predicted reliability corresponds to the optimal parameters (125.03 ppm dye concentration, 0.06 wt percent additive loading, and 132 kPa pressure).

Table 7
Validation results at 125 *mg/L*, an additive loading of 0.06 wt%, and an operating pressure of 132 kPa.

(Y)	experimental	predicated	% Error
Rejection	99.8200	98.200	1.6
Flux (kg/m^2 h)	44.500	43.8300	1.5

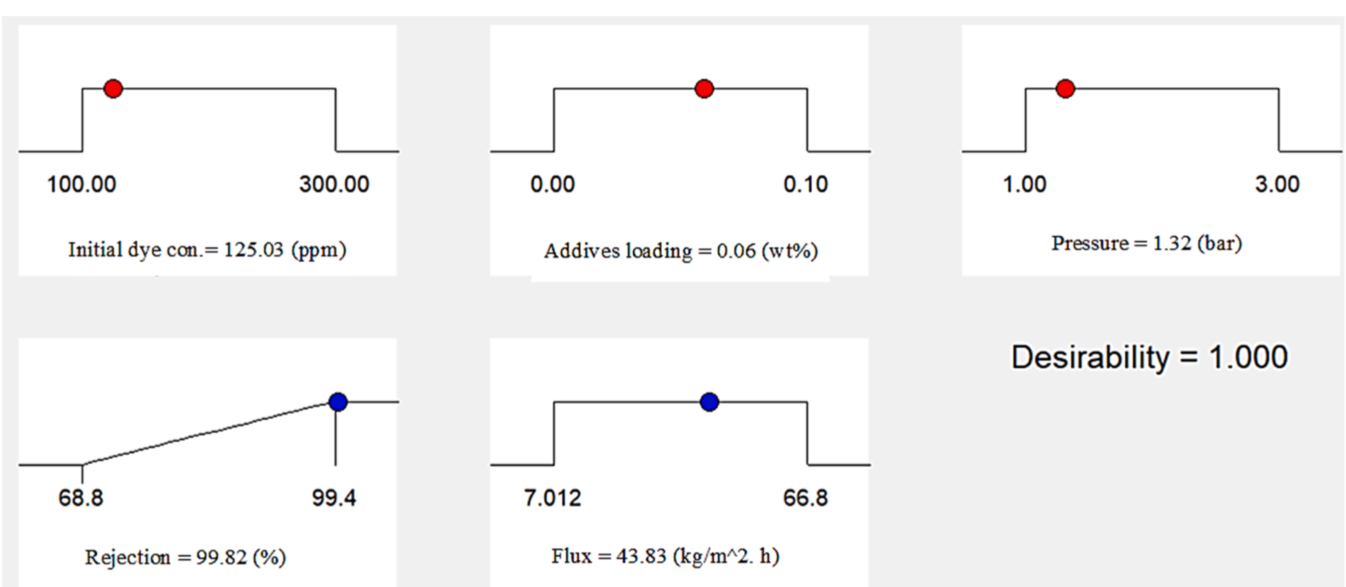

Fig. 10. Desirability ramp for three selected factors' numerical optimization.

- The robustness and accuracy of the model are confirmed by the close agreement between the experimental and projected values of flux (43.83 $kg/m^2 \cdot h$) and rejection (99.82%).

The integration of multi-objective optimization using desirability functions, which concurrently maximizes dye rejection and permeate flux, is what makes Fig. 10 innovative. This method offers a more dependable and practically applicable operating window with high predictive accuracy throughout the dataset, in contrast to traditional single-response optimization.

5. Comparison with previous study

Important developments in PES-based nanocomposite membranes are highlighted in Table 8, especially those that use TiO_2, Bi-based, and Fe-based nanoparticles. This review offers a holistic analysis of membrane fabrication processes, nanoparticle synergistic effects, and optimum operating parameters, in contrast to previous publications that mainly concentrate on single nanoparticle systems or isolated performance measures. With regard to permeability–selectivity trade-offs, antifouling behavior, and photocatalytic self-cleaning qualities in particular, this wider view makes it easier to identify performance enhancing methods.

6. Future scope and research directions

Although polyethersulfone (PES) membranes studded with Titanium Dioxide-Bismuth Ferrite nanoparticles (TiO_2-$BiFeO_3$), has shown promise in dye removal, there are still a number of unexplored research avenues. Future research should concentrate on increasing membrane production and assessing performance in pilot-scale and actual industrial wastewater settings, where operational variations and complicated pollutant matrices may affect separation effectiveness. To evaluate practical applications, long-term studies of membrane integrity, fouling behavior, and cleaning techniques are also crucial. In addition, optimizing nanoparticle dispersion, interfacial compatibility, and loading concentration is crucial to achieving an improved balance between permeability and selectivity. Advanced characterization techniques and modeling approaches could provide deeper insights into transport mechanisms and fouling dynamics. Furthermore, the incorporation of multifunctional properties, such as photocatalytic self-cleaning and antimicrobial activity, offers significant potential to enhance membrane lifespan and reduce operational costs [51,52]. Future work may also explore the integration of these nanocomposite membranes into hybrid treatment systems, combining membrane filtration with advanced oxidation or adsorption processes to improve overall treatment efficiency. Finally, the application of data-driven and machine learning approaches to optimize fabrication parameters and predict membrane performance represents a promising emerging direction [53].

7. Conclusion

This work showed how to optimize ultrafiltration (UF) performance for treated produced water (PW) using a PES/TiO_2–$BiFeO_3$ (PES/TBF) mixed matrix membrane in a methodical and statistically driven manner. The paper offers a novel quantitative knowledge of the independent and combined impacts of feed dye concentration, operating pressure, and nanoparticle loading on membrane performance by combining Response Surface Methodology (RSM) with ANOVA. This study makes a significant addition by showing that feed concentration has a relatively small influence on permeate flux and dye rejection, while nanoparticle additive content and operating pressure are the main determinants. High adjusted R^2 projected R^2 and sufficient precision values demonstrated the generated predictive models' great agreement with experimental data, demonstrating their dependability for process prediction and optimization. Significantly, at ideal conditions (0.06 wt

Table 8
Comparison with the previous study.

Study	Membrane Composition	Preparation Method	Target Dye	Operating Conditions	Flux (LMH)	Rejection (%)	Key Findings
[47]	PES/$BiFeO_3$	Phase inversion	MB	0.1–0.4 wt% NP; ~2–3 bar	~52.5	> 99	Enhanced hydrophilicity, antifouling, and dye rejection due to $BiFeO_3$ incorporation
[41]	PES/$BiFeO_3$	Phase inversion + RSM optimization	MB	0.25 wt%, 10 ppm, 2.57 bar	63.5	97.97	Optimized operating parameters significantly improved flux and rejection
[27]	PES/TiO_2–$BiFeO_3$	NIPS	Congo Red	0–0.1 wt% NP	~55	94.84	Improved permeability and self-cleaning via photocatalysis (ROS generation)
[48]	PES/TiO_2–Fe_2O_3	Phase inversion	NBB dye	Variable NP loading	~59	—	Improved antifouling and flux stability under visible light conditions
[49]	PES/Fe_2O_3–TiO_2	Surface modification	Organic/ biofoulants	Saline + light	~59	—	Significant reduction in fouling (RFR ↓ from 60% to 5%) due to photocatalytic activity
[50]	PES/ZnO/ biomass	Blending	Various dyes	—	—	—	Improved antifouling and adsorption capacity via hybrid organic–inorganic structure
This Work	TiO_2-$BiFeO_3$ NPs	Phase inversion + RSM optimization	CR dye	operating pressure (100–300 bar), (CR) dye concentration (0.1–0.3 g/L), nanoparticle loading (0–0.1 wt%).	Up to ~60 +	Up to ~99	Provides integrated analysis of nanoparticle synergy, operating conditions optimization, and structure–performance relationships

percent additive, 125 mg/L dye concentration, and 132 kPa), the improved PES/TBF membrane exhibited a high permeate flux of 43.8 $kg \cdot m^{-2} \cdot h^{-1}$ combined with a good dye rejection of 99.8%. These findings demonstrate how well membrane design boosted by nanoparticles may simultaneously improve selectivity and permeability. All things considered, this work advances the field by presenting an effective optimization framework along with improved membrane functionality, providing a viable and scalable method for high-performance dye removal in wastewater treatment applications.

CRediT authorship contribution statement

Hussain Ali Ibrahim: Writing – original draft, Resources, Methodology, Investigation, Formal analysis, Data curation, Conceptualization. **AbdulRazak Adnan A.:** Writing – review & editing, Writing – original draft, Validation, Software, Methodology, Investigation, Formal analysis, Data curation. **Mahmood Alhafadhi:** Investigation, Formal analysis, Data curation. **Mohammed Nabeel:** Resources, Investigation, Formal analysis. **Haidar Hasan Mohammed:** Validation, Investigation, Formal analysis, Data curation. **Mohammad A. Taher:** Validation, Software, Formal analysis, Data curation. **Mohammed A. Salih:** Resources, Investigation, Formal analysis. **Mohammed Ahmed Shehab:** Writing – review & editing, Writing – original draft, Resources, Methodology, Investigation, Formal analysis. **Khalid T. Rashid:** Writing – review & editing, Writing – original draft, Software, Resources, Methodology, Investigation, Formal analysis, Data curation.

Funding

This research received no external funding

Declaration of Competing Interest

The authors declare that they have no known competing financial interests or personal relationships that could have appeared to influence the work reported in this paper.

Appendix A. Supporting information

Supplementary data associated with this article can be found in the online version at doi:10.1016/j.dwt.2026.101781.

Data Availability

Data will be made available on request.

References

[1] Akbari A, Remigy JC, Aptel P. Treatment of textile dye effluent using a polyamide-based nanofiltration membrane. Chem Eng Process Process Intensif 2002;41(7):601–9. https://doi.org/10.1016/S0255-2701(01)00181-7.

[2] Keskin B, Ersahin ME, Ozgun H, Koyuncu I. Pilot and full-scale applications of membrane processes for textile wastewater treatment: a critical review. J Water Process Eng 2021;42:102172. https://doi.org/10.1016/j.jwpe.2021.102172.

[3] Raja RI, Rashid KT, Toma MA, AbdulRazak AA, Shehab MA, Hernadi K. A novel Polyethersulfone/Chamomile (PES/Chm) mixed matrix membranes for wastewater treatment applications. J Saudi Chem Soc 2024;28(2):101805. https://doi.org/10.1016/j.jscs.2023.101805.

[4] Johari NA, Hamzah MAAM, Yusof N, Abdullah N, Ismail AF, Lau WJ, et al. Efficient textile wastewater treatment by hybrid ultrafiltration membrane incorporated with novel tannin-modified metal-organic framework. J Environ Chem Eng 2025;13(2):115617. https://doi.org/10.1016/j.jece.2025.115617.

[5] Yahia Y, Rashid KT, Toma MA, Shakhir KS, Albayati TM, Saady NMC, et al. A novel green propolis (bee glue) nanoparticles mixed with poly (ether sulfone) ultrafiltration membrane for wastewater Eriochrome Black T (EBT) and Congo Red (CR) dye treatment. J Environ Chem Eng 2025;13(2):115913. https://doi.org/10.1016/j.jece.2025.115913.

[6] Solayman HM, Hossen MA, Aziz AA, Yahya NY, Hon L, Ching SL, et al. Performance evaluation of dye wastewater treatment technologies: a review. J Environ Chem Eng 2023;11(3):109610. https://doi.org/10.1016/j.jece.2023.109610.

[7] Nachiyar CV, Rakshi AD, Sandhya S, Jebasta NBD, Nellore J. Developments in treatment technologies of dye-containing effluent: a review. Case Stud Chem Environ Eng 2023;7:100339. https://doi.org/10.1016/j.cscee.2023.100339.

[8] Khader EH, Mohammed TJ, Albayati TM, Rashid KT, Saady NMC, Zendehboudi S. Green nanoparticles blending with polyacrylonitrile ultrafiltration membrane for antifouling oily wastewater treatment. Sep Purif Technol 2025;353(Part A):128256. https://doi.org/10.1016/j.seppur.2024.128256.

[9] Shen M, Zhao Y, Liu S, Hu T, Zheng K, Wang Y, et al. Recent advances on micro/nanoplastic pollution and membrane fouling during water treatment: a review. Sci Total Environ 2023;881:163467. https://doi.org/10.1016/j.scitotenv.2023.163467.

[10] Seah MQ, Chua SF, Ang WL, Lau WJ, Mansourizadeh A, Thamaraiselvan C. Advancements in polymeric membranes for challenging water filtration environments: a comprehensive review. J Environ Chem Eng 2024;12(3):112628. https://doi.org/10.1016/j.jece.2024.112628.

[11] Bakri MKB, Rahman MR. Introduction to recent developments and future opportunities for polymer nanocomposite membranes. Polym Nanocompos Membr Water Treat Desalin 2025:1–27. https://doi.org/10.1016/B978-0-443-23879-6.00001-4.

[12] Al Aani S, Wright CJ, Atieh MA, Hilal N. Engineering nanocomposite membranes: Addressing current challenges and future opportunities. Desalination 2017;401:1–15. https://doi.org/10.1016/j.desal.2016.08.001.

[13] Al Aani S, Gomez V, Wright CJ, Hilal N. Fabrication of antibacterial mixed matrix nanocomposite membranes using hybrid nanostructure of silver coated multi-walled carbon nanotubes. Chem Eng J 2017;326:721–36. https://doi.org/10.1016/j.cej.2017.06.029.

[14] Kadhim RJ, Al-Ani FH, Alsalhy QF. MCM-41 mesoporous modified polyethersulfone nanofiltration membranes and their prospects for dyes removal. Int J Environ Anal Chem 2023;103(4):828–48. https://doi.org/10.1080/03067319.2020.1865326.

[15] Hashmi Zubair, Idriss Ibrahim Maina, Gapsari Femiana, Samsuddin Norazanita, Bilad Muhammad Roil. The role of nanomaterials in enhancing membrane-based treatment for emerging contaminants: a review. ISSN 2772-8269 Sustain Chem Clim Action 2025;7:100092. https://doi.org/10.1016/j.scca.2025.100092.

[16] Kuvarega AT, Khumalo N, Dlamini D, Mamba BB. Polysulfone/N, Pd co-doped TiO_2 composite membranes for photocatalytic dye degradation. Sep Purif Technol 2018;191:122–33. https://doi.org/10.1016/j.seppur.2017.07.064.

[17] Leong S, Razmjou A, Wang K, Hapgood K, Zhang X, Wang H. TiO_2 based photocatalytic membranes: a review. J Membr Sci 2014;472:167–84. https://doi.org/10.1016/j.memsci.2014.08.016.

[18] Zhang B, Peng Y, Yao Y, Hong X, Wu Y. Constructing a composite microfiltration carbon membrane by TiO_2 and Fe_2O_3 for efficient separation of oil-water emulsions. Environ Sci Pollut Res Int 2023;30(40):92027–41. https://doi.org/10.1007/s11356-023-28728-x.

[19] Li N, Tian Y, Zhang J, Sun Z, Zhao J, Zhang J, et al. Precisely-controlled modification of PVDF membranes with 3D TiO_2/ZnO nanolayer: enhanced anti-fouling performance by changing hydrophilicity and photocatalysis under visible light irradiation. J Membr Sci 2017;528:359–68. https://doi.org/10.1016/j.memsci.2017.01.048.

[20] Rathna T, PonnanEttiyappan J. D. RubenSudhakar, Fabrication of visible-light assisted TiO_2-WO_3-PANI membrane for effective reduction of chromium (VI) in photocatalytic membrane reactor. Environ Technol Innov 2021;24:102023. https://doi.org/10.1016/j.eti.2021.102023.

[21] Ghadhban MY, et al. Optimal operational conditions of PLA/PBAT mixed matrix membrane for the treatment of oily wastewater. Eng Technol J 2024;42(9):1179–92. https://doi.org/10.30684/etj.2024.150993.1774.

[22] Rashid KT, Rahman SBA, Alsalhy QF. Optimum Operating Parameters for Hollow Fiber Membranes in Direct Contact Membrane Distillation. Arab J Sci Eng 2016;41:2647–58. https://doi.org/10.1007/s13369-016-2178-3.

[23] Abdulgader M, Yu QJ, Zinatizadeh AA, Williams P, Rahimi Z. Application of response surface methodology (RSM) for process analysis and optimization of milk processing wastewater treatment using multistage flexible fiber biofilm reactor. J Environ Chem Eng 2020;8(3):103797. https://doi.org/10.1016/j.jece.2020.103797.

[24] Li B, Yue R, Shen L, Chen C, Li R, Xu Y, et al. A novel method integrating response surface method with artificial neural network to optimize membrane fabrication for wastewater treatment. J Clean Prod 2022;376:134236. https://doi.org/10.1016/j.jclepro.2022.134236.

[25] Inger M, Dobrzyńska-Inger A, Rajewski J, Wilk M. The use of response surface methodology in ammonia oxidation reaction study. 2641315 J Chem 2019:1–8. https://doi.org/10.1155/2019/2641315.

[26] Boubakri A, Hafiane A, Bouguecha SAT. Application of response surface methodology for modeling and optimization of membrane distillation desalination process. J Ind Eng Chem 2014;20(5):3163–9. https://doi.org/10.1016/j.jiec.2013.11.060.

[27] Karunakaran A, Chaturvedi A, Ali J, Singh R, Agarwal S, Garg MC. Response surface methodology-based modeling and optimization of chromium removal using spiral-wound reverse-osmosis membrane setup. Int J Environ Sci Technol 2022;19:5999–6010. https://doi.org/10.1007/s13762-021-03422-y.

[28] Srivastava A, Singh R, Rajput VD, Minkina T, Agarwal S, Garg MC. A systematic approach towards optimization of brackish groundwater treatment using nanofiltration (NF) and reverse osmosis (RO) hybrid membrane filtration system. Chemosphere 2022;303:135230. https://doi.org/10.1016/j.chemosphere.2022.135230.

[29] Ibrahim HA, Rashid KT, AbdulRazak AA, Shehab MA, Salih MA, Al-lami M, et al. A novel poly(ether Sulfone) mixed matrix membranes infused with TiO_2-$BiFeO_3$

nanomaterials for the removal of toxic Congo red dye from textile wastewater. Chem Eng J Adv 2025;24:100867. https://doi.org/10.1016/j.ceja.2025.100867.
[30] Liu Y, Zhu J, Chi MS, Eygen GV, Guan K, Matsuyama H. Comprehensive review of nanofiltration membranes for efficient resource recovery from textile wastewater. Chem Eng J 2025;506:160132. https://doi.org/10.1016/j.cej.2025.160132.
[31] Ahmed FS, AbdulRazak AA, Alsaffar MA. Modelling and optimization of methylene blue adsorption from wastewater utilizing magnetic marble dust adsorbent: A response surface methodology approach. Mater Today Proc 2022;60:1676–88. https://doi.org/10.1016/j.matpr.2021.12.224.
[32] Ali NN, Alayan HM, AbdulRazak AA, Jalil RR. Modeling and optimizing phenol degradation in aqueous solution using post discharge DBD plasma treatment. Desalin Water Treat 2025;321:100993. https://doi.org/10.1016/j.dwt.2025.100993.
[33] Khalaf IH, Al-Sudani FT, AbdulRazak AA, Aldahri T, Rohani S. Optimization of Congo red dye adsorption from wastewater by a modified commercial zeolite catalyst using response surface modeling approach. Water Sci Technol 2021;83(6):1369–83. https://doi.org/10.2166/wst.2021.078.
[34] Ahmed N, Mir FQ. Box–Behnken design for optimization of iron removal by hybrid oxidation–microfiltration process using ceramic membrane. J Mater Sci 2022;57(32):15224–38. https://doi.org/10.1007/s10853-022-07567-0.
[35] Shakor ZM, AbdulRazak AA, Shuhaib AA. Optimization of process variables for hydrogenation of cinnamaldehyde to cinnamyl alcohol over a Pt/SiO_2 catalyst using response surface methodology. Chem Eng Commun 2022;209(6):827–43. https://doi.org/10.1080/00986445.2021.1922394.
[36] Zhang Y, Wang Y, Wang X, Zhang Z, Li S, Hu Y, et al. Construction of robust one-dimensional nanowire-regulated graphene oxide membranes for efficient dye/salt separation. J Membr Sci 2023;686:122027. https://doi.org/10.1016/j.memsci.2023.122027.
[37] Shihab JM, Rashid KT, Toma M. A review on membrane technology application for vegetable oil purification processes. Int J Food Eng 2022;18(10-11):655–77. https://doi.org/10.1515/ijfe-2022-0058.
[38] Abdelhamid AE, Elsayed AE, Naguib M, Ali EA. Effective dye removal by acrylic-based membrane constructed from textile fibers waste. Fibers Polym 2023;24(7):2391–9. https://doi.org/10.1007/s12221-023-00247-z.
[39] Elfiky AAEA, Mubarak MF, Keshawy M. Novel nanofiltration membrane modified by metal oxide nanocomposite for dyes removal from wastewater. Environ Dev Sustain 2024;26:19935–57. https://doi.org/10.1007/s10668-023-03444-1.
[40] Abdelhamid AE, Selim SE, Meligi GA. Antifouling ultrafiltration membranes based on acrylic fibers waste/nanochitosan for Congo red and crystal violet removal. Waste Dispos Sustain Energy 2024;6:511–27. https://doi.org/10.1007/s42768-024-00208-z.
[41] Chidambaram T, Oren Y, Noel M. Fouling of nanofiltration membranes by dyes during brine recovery from textile dye bath wastewater. Chem Eng J 2015;262:156–68. https://doi.org/10.1016/j.cej.2014.09.062.
[42] Jongkwan P, Jeong K, Baek S-S, Park S, Ligaray M, Chong TH, et al. Modeling of NF/RO membrane fouling and flux decline using real-time observations (http://DOI.org/) J Membr Sci 2019;576:66–77. https://doi.org/10.1016/J.MEMSCI.2019.01.031.
[43] Jawad SK, Rashid KT, Toma MA, Abdul Razak AA, Shehab MA, Ghadhban MY, et al. Optimal operating conditions of PES/$BiFeO_3$ mixed matrix membrane for treating dye-contaminated wastewater. Results Eng 2025;26:105246. https://doi.org/10.1016/j.rineng.2025.105246.
[44] Yahia Y, Rashid KT, Shehab MA, Abdul Razak AA, Ghadban MY, Al-lami M, et al. Treating wastewater contaminated with congo red (CR) dye using an optimized polyethersulfone/propolis (bee glue) PES/PRS ultrafiltration membrane. RSC Adv 2025;15(29):23174–86. https://doi.org/10.1039/D5RA03565A.
[45] Samari M, Zinadini S, Zinatizadeh AA, Jafarzadeh M, Gholami F. Performance evaluation of amino-functionalized mesoporous/PES nanofiltration membrane in anionic dye removal from aqueous solutions. Appl Water Sci 2022;12(12):263. https://doi.org/10.1007/s13201-022-01775-4.
[46] Pramono E, Umam K, Sagita F, Saputra OA, Alfiansyah R, Dewi RSS, et al. The enhancement of dye filtration performance and antifouling properties in amino-functionalized bentonite/polyvinylidene fluoride mixed matrix membranes. Heliyon 2023;9(1). https://doi.org/10.1016/j.heliyon.2023.e12823.
[47] Jawad SK, Rashid KT, Toma MA, AbdulRazak AA, Al-Bayati ADJ, Shakor ZM, et al. Fabrication, characterization, and modification of a novel polyethersulfone (PES) mix matrix membrane via $BiFeO_3$ as a hydrophilic additive to improve permeability and antifouling features. Environ Sci Pollut Res 2025;32:17563–84. https://doi.org/10.1007/s11356-025-36711-x.
[48] Hussein MM, Alsalhy QF, Gar Alalm M, El-Halwany MM. Optimization of Developed TiO_2 NWs-Fe_2O_3 Modified PES Membranes for Efficient NBB Dye Removal. ChemEngineering 2025;9:82. https://doi.org/10.3390/chemengineering9040082.
[49] Baniamerian H, Shokrollahzadeh S, Safavi MA, Ashori I, Angelidaki. Visible-light-activated Fe_2O_3–TiO_2 nanoparticles enhance biofouling resistance of polyethersulfone ultrafiltration membranes against marine algae *Chlorella vulgaris*. Sci Rep 2024;14:24831. https://doi.org/10.1038/s41598-024-76201-7.
[50] Boopathy G, Gangasalam A, Mahalingam A. Photocatalytic removal of organic pollutants and self-cleaning performance of PES membrane incorporated sulfonated graphene oxide/ZnO nanocomposite. J Chem Technol Biotechnol 2020;95:3012–23. https://doi.org/10.1002/jctb.6462.
[51] Zhang H, Quan X, Chen S, Zhao H, Zhao Y. Fabrication of photocatalytic membrane and evaluation its efficiency in removal of organic pollutants from water. Sep Purif Technol 2006;50(2):147–55. https://doi.org/10.1016/j.seppur.2005.11.018.
[52] Hazarika B, Ahmaruzzaman M, Santosh MS, Barceló D, Rtimi S. Advances in polymer-based nanocomposite membranes for water remediation: preparation methods, critical issues and mechanisms. J Environ Chem Eng 2023;11(6):111401. https://doi.org/10.1016/j.jece.2023.111401.
[53] De la Hoz-M J, Ariza-Echeverri EA, Vergara D. Exploring the role of artificial intelligence in wastewater treatment: a dynamic analysis of emerging research trends. Resources 2024;13(12):171. https://doi.org/10.3390/resources13120171.